Behaviour of high strength steel moment joints

A.M. Girão Coelho[a,b] and F.S.K. Bijlaard[a]

[a] Delft University of Technology, The Netherlands

[b] Institute of Computers and Systems Engineering of Coimbra, Portugal

The design of joints to European standard EN 1993 within the semi-continuous/partially-restrained philosophy is restricted to steel grades up to S460. With the recent development of high performance steels, the need for these restrictions should be revisited. The semi-continuous joint modelling can be adopted as long as the joint develops rotation capacity and behaves ductile. The research summarized in this paper focuses on moment joints with components made from high strength steel S460, S690 and S960 (yield stress of 460 N/mm², 690 N/mm² and 960 N/mm², respectively) to provide insight into the nonlinear behaviour of this joint type. Findings from a comprehensive research programme carried out in the Delft University of Technology are collected. The major contributions of this study are (i) the characterization of the rotational response in the framework of the component method, (ii) the validation of current EN 1993 specifications for joints and (iii) the ductility analysis of high strength steel moment joints. Test results show that the tested joints and components satisfy the current design provisions for stiffness and resistance and satisfy reasonable deformation demands.

Key words: Ductility, end plate connections, experimental testing, high strength steel, resistance, rotation capacity, stiffness, T-stub, web shear panel

1 Introduction

For decades the use of high performance steels was not very popular from the designers and manufacturers of steel structures standpoint. Designers claimed that the benefits of using high strength steel were little because there was no corresponding increase in the Young modulus as the yield stress increased, which could make problems of serviceability of structures being dominant. Manufacturers of steel structures, on the other hand, pointed at the higher costs of welding because of the special precautions that were required.

Furthermore there was much doubt about the toughness of the material and subsequently the ductility of the structures made from such classes of steel.

Recently, contractors have placed an emphasis on high performance construction materials to produce innovative structures. Light weight and thin elements are particularly attractive for architectural and aesthetic reasons as well as for the reduction of environmental impact of construction. The concrete industry rapidly developed high performance concrete to provide an answer to this demand. Gradually, these classes of concrete entered into the market of structures formerly dominated by steel. Sheet piles, lock doors and structures for industrial plants are examples of such a tendency. The way to face this competition is to develop strategies to better exploit the benefits of high performance steels.

High performance steels in construction, commonly classified as high strength steels, represent a family of steels with a yield stress of 460 N/mm^2 (S460) and above. The benefits of the use of these steels can be utilized in braced frames for which stiffness, in the form of deflections or drift limits for complying with serviceability limit states, does not govern design. Modern design codes adopt the semi-continuous/partially-restrained philosophy for the design of this type of framing in recognition of the economic benefits. This is a rational design method for plastically designed frames. It accounts for the interaction between members and joints. Thus, global frame analysis requires the characterization of the full nonlinear moment-rotation response of the joints, i.e. joints must be designed for strength, stiffness, rotation capacity and ductility (Figure 1). In particular, the important features of a joint in semi-continuous framing are that it is ductile and partial strength.

End plate bolted connections that are widely used in steel frames as moment-resistant joints between steel members usually fall in this category. The simplicity and economy associated to their fabrication and erection made this joint typology quite popular in steel-framed structures. In Europe, partial strength extended end plate connections are typical for low-rise buildings erected using welding at the shop and bolting on site. Rules for prediction of strength and stiffness of this joint configuration have been included in modern design codes as the EN 1993. No quantitative guidance for characterization of the ductility is yet available. Several authors, however, have recently highlighted the importance of designing structural joints for rotation capacity and ductility [Beg et al. 2004; Bjorhovde 2004b; Gioncu et al. 2000; Girão Coelho 2004]. The knowledge of the plastic

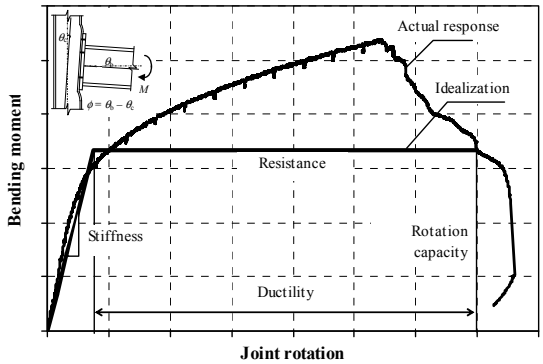

Figure 1: Moment-rotation response of a joint (definitions)

deformation supply of members and joints is particularly important for steel frames that experience abnormal loading conditions, such as fire and seismic events. In these extreme events, very high demands for local and global deformation are imposed on structural elements, connections and details. Connections between members, in particular, are the regions where the material is exposed to higher deformations and, consequently, they influence local ductility requirements and frame performance. EN 1993-1-8 [CEN 2005b] includes simple deemed-to-satisfy criteria to guarantee that the available deformation capacity is higher than the deformation demand of a specific joint. Derivation of such criteria can be found in Jaspart [1997] and Zoetemeijer [1990]. In the framework of the component method [Weynand et al. 1995], the rotational response of the joint is generated from the deformation behaviour of the individual components (e.g. panel zone, end plate in bending, welds, etc.). Joints should be designed such that inelastic actions are concentrated in those components that provide high ductility and satisfy high deformation demands. This imposes ductility and deformation demands to the joint that strongly depend on the geometry, loading conditions and, more particularly, on the material characteristics. Conventional steels (yield stress < 460 N/mm^2) are characterized by good or satisfactory deformability and ductility properties.

Traditionally, the design of structures fabricated from high strength steel is essentially based on an elastic concept. Part 1-12 of EN 1993 [CEN 2005c] (EN 1993-1-12) presently forbids elastic-plastic global structural analysis with plastified sections and/or joints acting as plastic hinges, because there is no background research work that shows that these elements and joints accommodate plastic deformations and are ductile. With the recent breakthroughs in steel making technologies that have produced high strength steels with

enhanced tensile mechanical properties, particularly in terms of deformability and ductility, the need for these restrictions have to be discussed.

The main topics of this paper are moment-resisting bolted (major axis) connections joining I-sections in high strength steel-framed structures and the characterization of their rotational behaviour in the framework of the component method [Weynand et al. 1995]. Findings from a number of recent research investigations into the behaviour of high strength steel beam-to-column joints and key components are collected. Currently used EN 1993 design criteria for joints are revisited in the light of the available experimental results.

2 Characterization of the moment-rotation response of joints in the framework of the component method

Beam-to-column joints consist of a web panel and one or two connections (one or two sided joint configuration). The web panel zone is the region within the column web and flanges into which the beams are framed. The connection is the location where two members are interconnected and where the set of physical components that mechanically fasten the connected elements are located.

The behaviour of a steel beam-to-column joint is represented by a moment-rotation (M-Φ) curve, as already explained. The rotational deformation Φ of a joint results from the in-plane bending M, and is the sum of the shear deformation of the column web panel zone γ, and the connection deformation ϕ ($\Phi = \phi + \gamma$). The deformation of the connection includes the deformation of the fastening elements (bolts, end plate, etc.) and the load-introduction deformation of the column web. It results in a relative rotation between the beam and column axes, θ_b and θ_c, which is equal to:

$$\phi = \theta_b - \theta_c \tag{1}$$

according to Figure 1, and provides a flexural deformability curve M-ϕ. This deformability is only due to the couple of forces F_b transferred by the flanges of the beam that are statically equivalent to the bending moment M acting on the beam. The shear deformation of the column web panel is associated with the force V_{wp} acting in this panel and leads to a relative rotation γ between the beam and column axes. A shear deformability curve V_{wp}-γ

may then be defined. The shear action in the panel is related to the internal actions on the joint by means of the transformation parameter β [Girão Coelho 2004; Jaspart 1997]:

$$V_{wp} = \beta M/z \tag{2}$$

whereby z is the lever arm [CEN 2005b]. Conservative values for parameter β, neglecting the effect of the shear force in the column are suggested in EN 1993-1-8: (i) $\beta = 1$ in the case of one sided joints, (ii) $\beta = 2$ in the case of two sided joints with equal but unbalanced end bending moments and (iii) $\beta = 0$ in the case of two sided joints with balanced end bending moments. The global moment-rotation response of the joint is then obtained by summing the contributions of rotation of the connection ϕ and of the shear panel γ ($\Phi = \phi + \gamma$).

Current design practice adopts the so-called component method for the prediction of the rotational behaviour of beam-to-column joints. For the purposes of simplicity, any joint can be subdivided into three different zones: tension, compression and shear. Within each zone, several sources of deformability can be identified, which are simple elemental parts (or "components") that contribute to the overall response of the joint. From a theoretical point of view, this methodology can be applied to any joint configuration and loading conditions provided that the basic components are properly characterized. The design basis consists of first identifying all active components for a given structural joint, then to establish the individual component force-deformation response and finally assembling those elements in form of a mechanical model made up of extensional springs and rigid links. This spring assembly is treated as a structure whose force-deformation behaviour is used to generate the moment-rotation curve of the full joint.

The basic layout of a bare steel extended end plate connection is illustrated in Figure 2a. For the computation of the joint rotational stiffness, the active joint components for this configuration, according to EN 1993-1-8, are: column web in shear (cws or wp), column web in compression (cwc), column web in tension (cwt), column flange in bending (cfb), end plate in bending (epb), and bolts in tension (bt). The welds connecting the end plate and the beam are not taken into account for computation of the rotational stiffness, as well as components beam web and flange in compression (bfc) and beam web in tension (bwt). Each component is characterized by a nonlinear force-deformation response, which can be obtained by means of experimental tests or analytical models. These individual components

are assembled into a mechanical model in order to evaluate the moment-rotation response of the whole joint. The EN 1993 spring model is represented in Figure 2b [Weynand et al. 1995]. The springs are combined in series or in parallel depending on the way they interplay with each other. Springs in series are subjected to the same force whilst parallel springs undergo the same deformation. Alternative spring and rigid link models are proposed in literature, as the "Innsbruck model" proposed by Huber and Tschemmernegg [1998]. Essentially, they share the same basic components but assume different component interplay.

Formulae required to determine the stiffness coefficient and the resistance of the basic components are provided in EN 1993-1-8. The code does not provide an anticipated value of the deformation capacity of the basic components.

2.1 Evaluation of the key moment-rotation parameters according to EN 1993

The design treatment presented herein is limited to the case of bolted end plate joints. Initial rotational stiffness is determined on the basis of the spring model illustrated in Figure 2b. The use of equilibrium and compatibility conditions, coupled with considerations of stiffness and deformation of the individual components, to produce an expression for the initial rotational stiffness is fully described in Girão Coelho [2004].

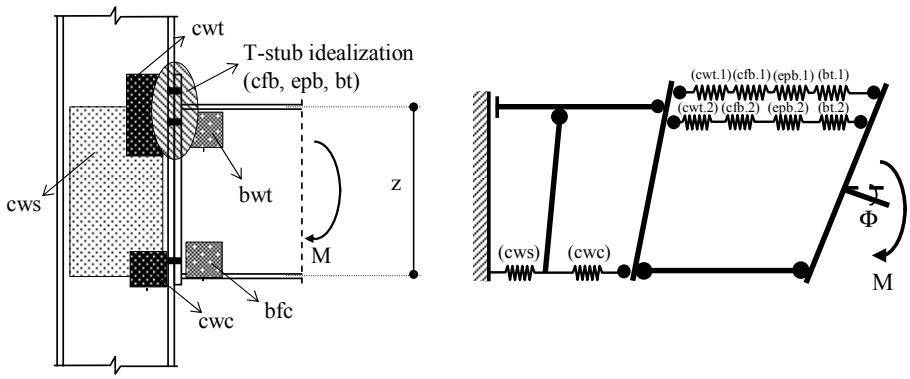

a) Identification of the basic components b) Mechanical model adopted in EN 1993

Figure 2: Representation of an extended end plate bolted connection with two bolt rows in tension (one sided steel joint configuration) and identification of the basic components

The resulting expression is:

$$S_{j.ini} = \frac{z^2}{1/k_{ec} + 1/k_{et}} \tag{3}$$

whereby k_{ec} and k_{et}: stiffness of the assembly of components in the compression/shear zone and in the tension zone, respectively. Use of Eq. (3) requires values to be ascribed to the terms k_{ec} and k_{et} [CEN 2005b]. The relevant formulae are set out below:

$$k_{ec} = \frac{1}{\frac{1}{k_{cws}} + \frac{1}{k_{cwc}}} \tag{4}$$

$$k_{et} = \frac{\sum_r k_{et,r} h_r}{z} \quad \text{and} \quad k_{et,r} = \frac{1}{\frac{1}{k_{cwt,r}} + \frac{1}{k_{cfb,r}} + \frac{1}{k_{epb,r}} + \frac{1}{k_{bt,r}}} \tag{5}$$

$$z = \frac{\sum_{r=1}^{n} k_{et,r} h_r^2}{\sum_{r=1}^{n} k_{et,r} h_r} \tag{6}$$

whereby h_r is the distance between bolt-row r and the centre of compression and $k_{et,r}$ is the effective stiffness coefficient for bolt-row r taking into account the stiffness coefficients of the individual components [CEN 2005b].

End plate joints transmit moment by coupling tension force(s) in the bolts with compression at the opposite flange. The joint design flexural resistance, $M_{j,Rd}$, in the absence of an axial force, is then calculated from simple equilibrium considerations:

$$M_{j,Rd} = \sum_{r=1}^{n} F_{tr,Rd} h_r \tag{7}$$

where $F_{tr,R}$ is the resistance of bolt row r in the tension zone (subscript "d" indicates "design value") that is taken as the least of the following values:

$$F_{tr,Rd} = \min\left(F_{cwt,r,Rd}, F_{cfb,r,Rd}, F_{epb,r,Rd}, F_{bwt,r,Rd}, F_{bt,r,Rd}\right) \tag{8}$$

where $F_{x,r,R}$ is the resistance of component x (see Figure 2b) at bolt row r. The values of $F_{tr,Rd}$ are calculated starting at the top row and working down. Bolt rows below the current row are ignored. Each bolt row is analysed first in isolation and then in combination with the successive rows above it. The procedure can be summarized as follows [CEN 2005b; Faella et al. 2000; Girão Coelho 2004]:

1. Compute the plastic resistance of bolt row 1 omitting the bolt rows below:

$$F_{t1,Rd} = \min\left(F_{cwt,1,Rd}, F_{cfb,1,Rd}, F_{epb,1,Rd}, F_{bwt,1,Rd}, F_{bt,1,Rd}\right) \tag{9}$$

2. Compute the plastic resistance of bolt row 2 omitting the bolt rows below:

$$\begin{aligned} F_{t2,Rd} = \min\big(&F_{cwt,2,Rd}, F_{cfb,2,Rd}, F_{epb,2,Rd}, F_{bwt,2,Rd}, F_{bt,2,Rd}, F_{cwt,(1+2),Rd} - F_{t1,Rd}, \\ &F_{cfb,(1+2),Rd} - F_{t1,Rd}, F_{epb,(1+2),Rd} - F_{t1,Rd}, F_{bwt,(1+2),Rd} - F_{t1,Rd}, F_{bt,(1+2),Rd} - F_{t1,Rd}\big) \end{aligned} \tag{10}$$

and so forth. The above values should be reduced, if necessary, to ensure that the following conditions are satisfied:

$$\Sigma F_{tr,Rd} \le V_{wp,Rd}/\beta \quad \text{and} \quad \Sigma F_{tr,Rd} \le \min\left(F_{cwc,Rd}, F_{bfc,Rd}\right) \tag{11}$$

EN 1993-1-8 also gives some guidelines to predict the rotation capacity: a bolted end plate joint may be assumed to have sufficient rotation capacity for global plastic analysis, provided that both of the following criteria are satisfied: (i) the moment resistance of the joint is governed by the resistance of either the column flange or the end plate in bending and (ii) the maximum (subscript "max") thickness t of either the column flange or end plate – not necessarily the same component as (i) – fulfils:

$$t \le t_{max} = 0.36\phi_b\sqrt{f_{u,b}/f_y} \tag{12}$$

where ϕ_b is the bolt diameter; $f_{u,b}$: tensile strength of the bolt and f_y is the yield stress of the relevant basic component. These guidelines are yet insufficient to ensure adequate ductility in partial strength joints [Jaspart 1997; Beg et al. 2 Girão Coelho 2004].

2.2 *Modelling of bolt row behaviour through equivalent T-stubs*

In the case of thin end plates, the joint rotation mainly comes from the end plate deformation on the tension side that can be idealized as a T-stub [Aggerskov 1977; CEN 2005b; Packer and Morris 1977; Yee and Melchers 1986; Zoetemeijer 1974]. Figure 3 identifies the T-stub that accounts for the deformation of the column flange and the end plate in bending in the particular case of an extended end plate bolted connection. In this particular case, since the column flange is unstiffened, the T-stub on the column side is orientated at right angles to the end plate T-stub [Yee and Melchers 1986].

The T-stub idealization of the tension zone of a connection consists in substituting this zone for T-stub sections of appropriate effective length b_{eff} (Figure 4). These T-stub sections are connected by their flange to a rigid foundation (half-model) and subjected to a uniformly distributed force acting on the web plate [Girão Coelho 2004]. The extension of the end plate and the portion between the beam flanges are modelled as two separate equivalent T-stubs (Figure 4). On the column side, two situations have to be analysed: (i) the bolt rows act individually or (ii) the bolt rows act in combination (Figure 4).

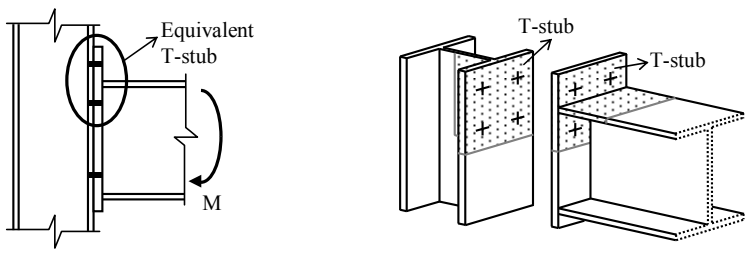

a) Unstiffened extended end plate connection: T-stub identification and orientation

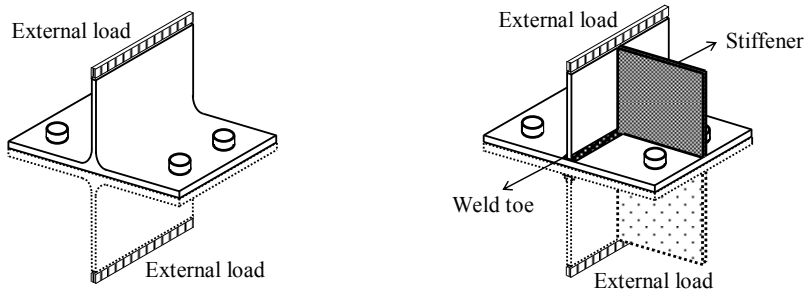

b) Model for the column flange side c) Model for the end plate side

Figure 3: T-stub identification and representation

The effective length of a T-stub is a notional width and does not necessarily represent any physical length of the flange. b_{eff} represents the width of the plate that contributes to load transmission and depends on the load level (elastic, yielding or near fracture). Therefore, it must be defined with respect to the key performance measures of initial elastic stiffness, plastic resistance and deformation capacity.

Zoetmeijer [1974] successfully introduced the T-stub concept in the context of the resistance of end plate connections. The effective length, in this case, accounts for all possible yield line mechanisms, either on the column side or the end plate side. It is defined by establishing the equivalence, in the plastic failure condition, between a beam model and the actual plate behaviour where collapse occurs due to the development of a yield line mechanism. EN 1993-1-8 presents expressions for evaluation of the effective length. In line with the upper bound method of plastic analysis, the value leading to the lowest plastic resistance has to be adopted, provided that it does not exceed the actual flange width. Typical observed yield-line patterns in thin end plates are shown in Figure 5, for the case of an end plate with one bolt row below the tension beam flange. For thicker end plates, the patterns may not develop fully as the bolt elongation behaviour may

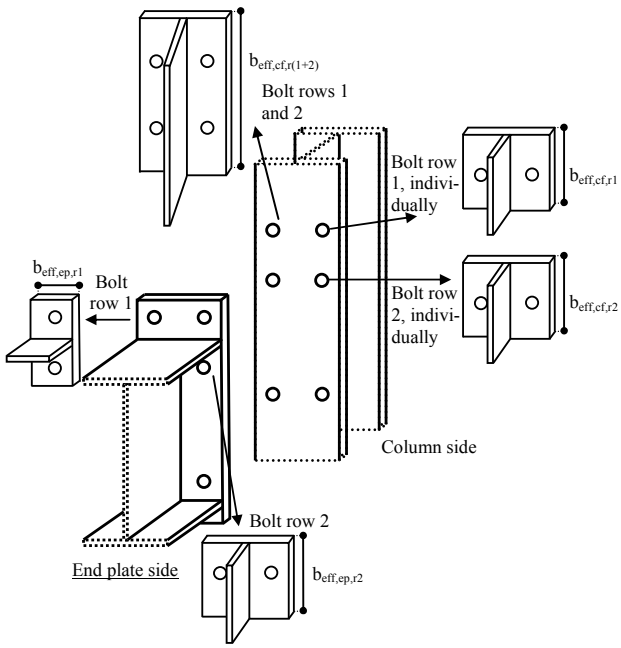

Figure 4: T-stub idealization of an extended end plate bolted joint with two bolt rows in tension

govern the overall response. For end plates with more than one bolt row below the tension beam flange, the cases of individual and combined bolt row behaviour have to be taken into consideration.

The main behavioural aspects of the T-stub as a standalone configuration have been widely investigated over the past thirty years, both experimentally and theoretically. Literature review on this topic can be found in Girão Coelho [2004]. As a result, the structural response of this connection configuration is thoroughly known in the elastic and plastic ranges, and appropriate design rules for the prediction of the main characteristics of the force-deformation curve have been assessed and included in EN 1993-1-8.

The code provides design rules for the evaluation of elastic stiffness $k_{e,0}$ and plastic resistance $F_{Rd,0}$, based on elastic theories [Jaspart 1991, 1997; Yee and Melchers 1986] and pure plastic theories [Packer and Morris 1977; Zoetemeijer 1974], respectively. The initial stiffness $k_{e,0}$ is evaluated as follows:

$$k_{e,0} = \frac{1}{2E \times 0.9 b_{eff} \left(t/m\right)^3 + 1.6 E A_s / L_b} \tag{13}$$

where E is the Young modulus of steel, t is the T-stub flange thickness, m is the distance between the bolt axis and the section corresponding to the "potential" plastic hinge at the flange-to-web connection, A_s is the tensile stress area of a bolt and L_b is the conventional

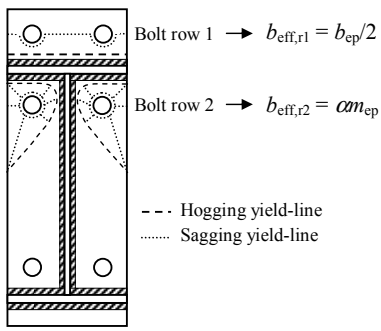

a) Plot

b) Illustration: spec. FS1b [Girão Coelho 2004]

Figure 5: Typical yield-line pattern in thin extended end plates with two bolt rows in tension

bolt length. According to EN 1993-1-8, $m = d - \zeta s$, where d is the length between the bolt axis and the face of the T-stub element web, ζ is a coefficient taken as 0.8 and $s = r$ or $s = \sqrt{2}a_w$, for hot rolled profiles and welded plates as T-stub, respectively; r is the fillet radius of the flange-to-web connection and a_w is the throat thickness of the fillet weld.

The plastic resistance is taken as the smallest value among the three possible plastic failure modes (Figure 6), i.e. $F_{Rd,0} = \min(F_{1,Rd,0}, F_{2,Rd,0}, F_{3,Rd,0})$, where:

$$F_{1,Rd,0} = 4M_{f,Rd}/m \tag{14}$$

$$F_{2,Rd,0} = \frac{2M_{f,Rd} + 2B_{Rd}n}{m+n} \tag{15}$$

$$F_{3,Rd,0} = 2B_{Rd} \tag{16}$$

The plastic flexural resistance of the T-flanges, $M_{f,Rd}$, is given by:

$$M_{f,Rd} = \frac{t^2}{4} f_{y,f} b_{eff} \tag{17}$$

where $f_{y,f}$ is the yield stress of the T-flanges and n is the effective edge distance. n is taken as the minimum value of e (distance between the bolt axis and the tip of the flanges) and $1.25m$, i.e. $n = \min(e, 1.25m)$. B_{Rd} is the "plastic" (design) resistance of a single bolt in tension.

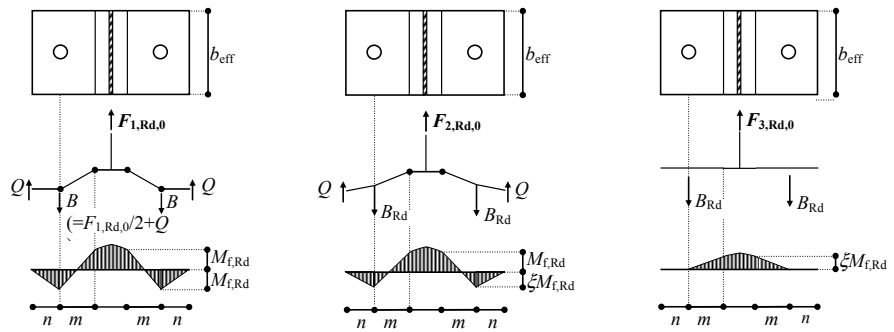

a) Flange plastic mechanism (type-1)

b) Combined bolt/flange mechanism (type-2; $\xi \leq 1$)

c) Bolt mechanism (type-3; $\xi \leq 1$)

Figure 6: Collapse mechanism typologies of a single T-stub connection at plastic conditions and distribution of internal actions

EN 1993-1-8 assumes elastic-perfectly plastic behaviour of the T-stub, with some implicit criteria to avoid brittle fracture. Consequently, the strain hardening and geometric nonlinear effects are neglected. Concerning the ductility, the code presents some qualitative principles based on the main contributions of the T-stub deformation: the ductility is infinite if the bending deformation of the flanges governs the plastic mechanism; should the bolt determine collapse, the ductility is limited.

Experimental characterization of the force-deformation response

Research into the behaviour of bolted T-stub connections made from welded plates has been undertaken at the Delft University of Technology. All the pertinent results and conclusions can be found in Girão Coelho [2004]. Of particular interest was the testing of seven specimens using high strength steel S690 and the comparison of results using EN

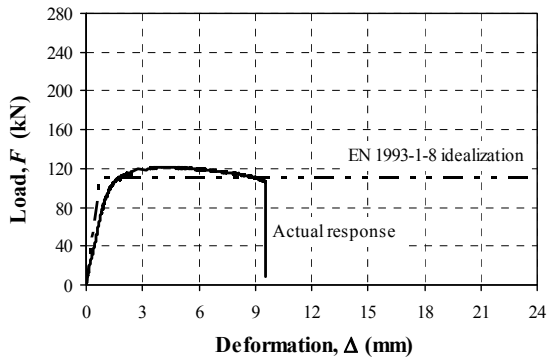

a) Normal bolts compared to plate thickness (M12 bolts in 10 mm S690 plates)

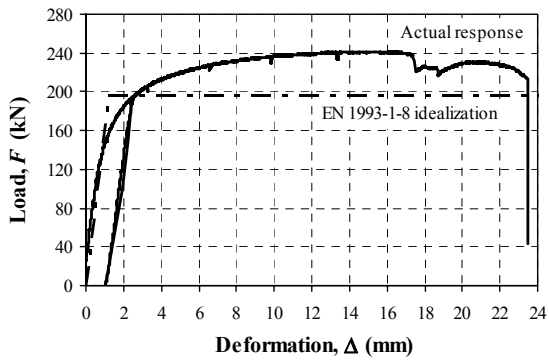

b) Large bolts compared to plate thickness (M20 bolts in 10 mm S690 plates)

Figure 7: Force-deformation response of T-stub connections tested by the author [2004]

1993-1-8. The observed failure modes involved combined bending and tension bolt fracture in nineteen specimens, stripping of the nut threads bolt fracture in one specimen, and combined cracking of the plate material in the heat affected zone and subsequent bolt fracture in one specimen that employed very large bolts in comparison with the plate thickness (WT57_M20). Figure 7 shows such comparisons. The model adopted in the code is accurate at representing the actual behaviour.

3 Behaviour of high strength steel end plate connections

3.1 Experimentally determined moment-rotation characteristics

A programme of experimental work was carried out in order to obtain moment-rotation characteristics for bolted end plate connections made from high strength steel. A general view of the test rig is shown in Figure 8. The connection details are given in Figure 9, and Table 1 contains details of the actual tests carried out. Extended end plate (EEP) and two different flush end plate configurations (F1EP and F2EP) were tested (Figure 9a). The relevant details of the test specimens are given in Figure 9b. Bolts were hand-tightened to give a snug fit in all sets. The actual mechanical properties for the end plates and bolts are also given in Table 1 (f_y is the yield stress; f_u is the tensile stress; $\rho_y = f_y/f_u$ is the yield ratio; ε_f is the strain at rupture load). The complete documentation of the work can be found in Girão Coelho and co-authors [2004, 2006, 2007].

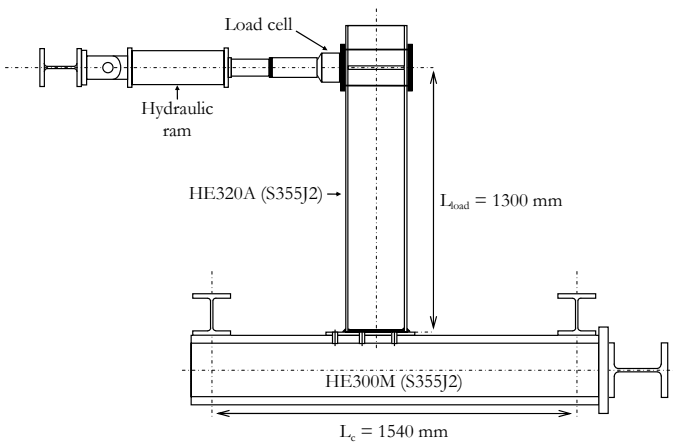

Figure 8: Test setup for extended end plate specimens

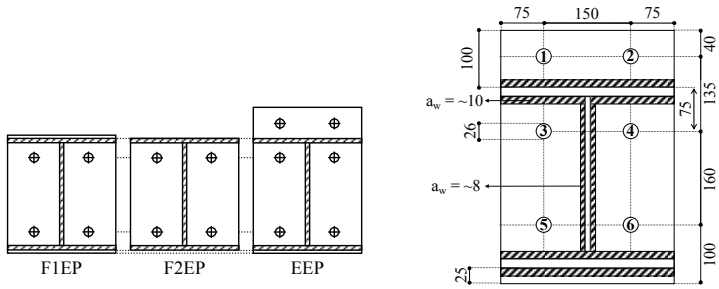

a) Configurations b) End plate dimensions

Figure 9: End plate configurations and dimensions

The specimens were designed to trigger failure in the assembly end plate-bolts in the tension zone without development of the full plastic moment capacity of the beam (partial strength joint). Beam and column sections were of class 1 [CEN 2005a]. An end plate connection comprises several critical components, as explained above. This study focuses on the single contribution of the assembly end plate-bolts in the tension zone. These components are modelled as equivalent T-stubs. Previous work [Faella et al. 2000; Girão Coelho 2004; Zoetemeijer 1990] on similar connection details has shown that the deformation characteristics primarily depends on (i) the connection geometry, particularly the ratio between the end plate thickness t_{ep}, and the bolt diameter ϕ_b, (ii) the assurance of a good material ductility for plate and bolts, (iii) the ratio between the resistance of the plate and the bolt and (iv) the welding quality.

Some typical moment-rotation results are shown in Figures 10 and 11. The behaviour observed is generally nonlinear. An initial stiff (linear) phase is followed by a second (quasi-linear) phase of much reduced stiffness. This curve defines the following structural properties (see Figure 10):

1. initial rotational stiffness $S_{j,ini}$;
2. post-yield rotational stiffness $S_{j,p-l}$;
3. "pseudo-plastic" resistance $M_{j,R}$ [Jaspart 1997], which is taken as the intersection between the two above characteristic behavioural phases;
4. maximum resistance $M_{j,max}$;
5. rotation capacity ϕ_C, defined at the rotation level for which failure of one or more components occurred.

Table 1: Details of test specimens

Test ID	Column		Beam		End plate					Bolt		
(For Test ID, see [Girão Coelho and Bijlaard 2007])	Section	Grade	Section	*Grade*	t_{ep} (mm)	Grade	$f_{y,ep}$ (MPa)	ρ_y	ε_f	ϕ_b (mm)	Grade	$f_{u,b}$ (MPa)
F1EP_15_1	HE300M	S355	HE320A	S355	15.30	S460	483	0.84	0.175	24	12.9	1413
F2EP_15_1	HE300M	S355	HE320A	S355	15.30	S460	483	0.84	0.175	24	12.9	1413
EEP_15_1	HE300M	S355	HE320A	S355	15.25	S460	483	0.84	0.175	24	8.8	940
F1EP_15_2	HE300M	S355	HE320A	S355	14.75	S690	774	0.95	0.186	24	12.9	1413
F2EP_15_2	HE300M	S355	HE320A	S355	14.64	S690	774	0.95	0.186	24	12.9	1413
EEP_15_2	HE300M	S355	HE320A	S355	14.62	S690	774	0.95	0.186	24	12.9	1413
F1EP_10_2	HE300M	S355	HE320A	S355	10.15	S690	698	0.93	0.175	24	12.9	1413
F2EP_10_2	HE300M	S355	HE320A	S355	10.25	S690	698	0.93	0.175	24	12.9	1413
EEP_10_2a	HE300M	S355	HE320A	S355	10.10	S690	698	0.93	0.175	24	12.9	1413
EEP_10_2b	HE300M	S355	HE320A	S355	10.10	S690	698	0.93	0.175	24	8.8	940
F1EP_10_3	HE300M	S355	HE320A	S355	10.00	S960	952	0.91	0.154	24	12.9	1413
F2EP_10_3	HE300M	S355	HE320A	S355	10.00	S960	952	0.91	0.154	24	12.9	1413
EEP_10_3	HE300M	S355	HE320A	S355	10.00	S960	952	0.91	0.154	24	12.9	1413
F2EP_10_2(M27)	HE300M	S355	HE320A	S355	10.05	S690	698	0.93	0.175	27	8.8	1013
EEP_10_2(M27)	HE300M	S355	HE320A	S355	10.10	S690	698	0.93	0.175	27	8.8	1013
F2EP_10_3(M27)	HE300M	S355	HE320A	S355	10.00	S960	952	0.91	0.154	27	8.8	1013
EEP_10_3(M27)	HE300M	S355	HE320A	S355	10.03	S960	952	0.91	0.154	27	8.8	1013
FS4 (a&b) [*Girão Coelho 2004*]	*HE340M*	*S355*	*IPE300*	*S355*	*10.06*	*S690*	*699*	*0.94*	*0.174*	*20*	*8.8*	*917*

The characteristics of these curves for the several test details are set out in Table 2. The failure modes of the specimens are also indicated in the table: (i) mode A: cracking of the end plate in the heat affected zone, (ii) mode B: bolt-thread stripping and (iii) mode C: bolts in tension. The response for representative test specimens is given in Figure 11. Several conclusions can be drawn from the analysis of these graphs and the structural properties in Table 2:

1. The rotational stiffness of the joints increases with the end plate thickness; because this property mainly depends on the Young modulus, there are no relevant variations with the plate steel grade.
2. The moment resistance enhances with the end plate thickness and steel grade.
3. The rotation capacity decreases with the thickness of the end plate; in general, it also decreases with the plate steel grade, though this variation is also linked to the governing failure mode.
4. The behaviour of the two flush end plate configurations is identical over the entire elastoplastic range (Figure 11a).
5. The behaviour of extended end plate joints is much stiffer than "parent" flush end plate configurations; moment resistance is also larger but the deformation capacity is smaller (Figure 11a).
6. The joint performance, in terms of resistance and stiffness, with bolts M24 grade 12.9 and bolts M27 grade 8.8 is equivalent; however, from a ductility point of view, bolt grade 8.8 should be taken. Bolts 12.9 exhibited very limited ductility and hardly any deformation in bending. In fact, in some cases (e.g. specimens with extended end plates) failure of the bolt occurred due to excessive rotation near the bolt head. Therefore, a strong recommendation against the use of this bolt grade is made.

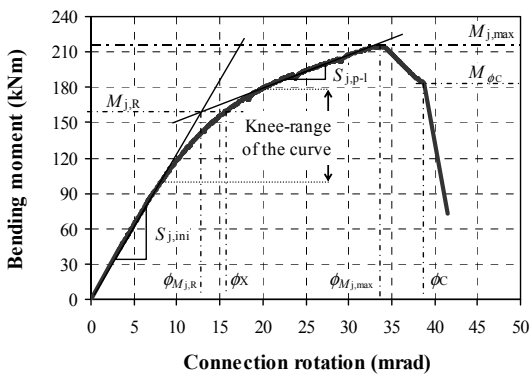

Figure 10: Typical moment-rotation response (e.g. F2EP_15_2)

The usual bolt diameter/end plate thickness combination for mild steel grades (e.g. bolts M24 in 15 mm plates) was checked for cases where high strength steel was present. Alternatively, the test programme included M27 8.8 bolts in 10 mm end plates, to check whether the overall ductility improved. In the latter case, very strong bolts were used in relatively thin end plates. The results however were rather disappointing since the rotation capacity did not increase as expected. The overall behaviour was dominated by cracking of the plate in the heat affected zone.

3.2 *Verification of EN 1993 predictions on test results*

The design of joints made from high strength steel up to S700 is covered in EN 1993-1-12, as mentioned above. This code does not allow the design of high strength steel joints within the semi-continuous concept. Experiments have however shown that yielding of the

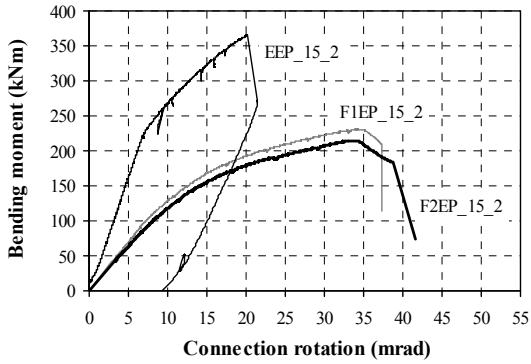

a) 15 mm end plates, S690

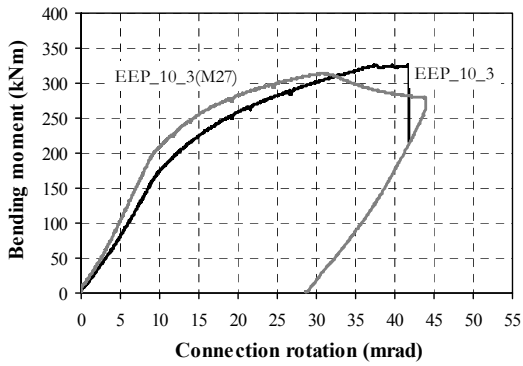

b) 10 mm extended end plates, S960

Figure 11: Moment-rotation curves for specimens employing S690 and S960

Table 2: Experimental characteristics of the moment-rotation curves

Test ID	**Stiffness** (kNm/mrad)		**Resistance** (kNm)		**Rotation capacity** (mrad)		**Failure mode**
(For Test ID, see [Girão Coelho and Bijlaard 2007])	$S_{j,ini}$	$S_{j,p-l}$	$M_{j,R}$	$M_{j,max}$	$\phi_{M_{j,max}}$	ϕ_C	
F1EP_15_1	18.4	0.18	192	198	33	33	Mode A
F2EP_15_1	12.7	2.1	128	172	32	40	Mode A
EEP_15_1	30.0	3.3	270	326	28	28	Mode B
F1EP_15_2	14.1	2.6	175	231	34	37	Mode C
F2EP_15_2	12.3	2.6	160	215	33	39	Mode C
EEP_15_2	35.3	9.7	245	366	20	20	Mode C
F1EP_10_2	7.8	1.9	95	142	39	46	Mode A
F2EP_10_2	7.2	1.4	89	117	35	41	Mode A
EEP_10_2a	17.2	3.2	173	244	36	45	Mode A
EEP_10_2b	19.9	5.4	188	252	37	46	Mode A
F1EP_10_3	9.3	–	171	201	46	46	Mode C
F2EP_10_3	8.0	0.8	155	176	52	–	Mode C
EEP_10_3	20.7	4.0	235	326	38	38	Mode C
F2EP_10_2(M27)	7.2	1.3	98	130	38	38	Mode A
EEP_10_2(M27)	23.2	3.4	195	266	30	52	Mode A
F2EP_10_3(M27)	10.9	1.9	123	173	42	67	Modes A&C
EEP_10_3(M27)	23.0	3.7	253	314	31	44	Mode A
FS4a	16.2	0.8	166	185	38	62	Mode C
FS4b	17.1	0.7	163	188	44	64	Mode C

end plate also occurs when employing high strength steel S690 or S960. Still, the adoption of this type of structural modelling for global analysis is only adequate if the joint develops sufficient rotation capacity so that a ductile failure mechanism of the whole structure can be formed prior to fracture of the joint.

Literature shows that end plate connections can achieve rotation capacity provided that the end plate is a "weak link" relative to the bolts [Girão Coelho 2004; Zoetemeijer 1990]. The conclusions however were validated for mild steel grades. Current tests employ end plates and bolts with similar mechanical properties, in terms of yield stress and yield ratio. It has to be investigated whether this influences the above premises.

In this section, a comparison between test results and current EN 1993-1-8 design provisions is undertaken for high strength steel. The code gives quantitative rules for the prediction of the joint flexural plastic resistance and initial stiffness. These structural properties are evaluated below by using the actual geometrical and mechanical properties [Girão Coelho 2004; Girão Coelho and Bijlaard 2006, 2007]. The recommendations on rotation capacity are also verified to investigate if there is enough rotation capacity according to EN 1993-1-8. The provisions are compared with the test results below. The partial safety factors γ_M are taken as unitary.

Table 3 shows such comparisons (subscripts "EC3" and "exp", respectively). The code overestimates structural stiffness properties (average ratio = 1.626 and coefficient of variation = 0.15). This is in line with experimental evidence from connections made from mild steels [Girão Coelho 2004]. The predictions for resistance compare well with test results (average ratio = 0.982 and coefficient of variation = 0.13). The authors have found that T-stub idealization of end plate behaviour is still a reliable approach, particularly in the pure plastic domain, even when end plates are made from high strength steel. The code recommendations on rotation capacity are also verified.

The following general observations are also made:

1. Test F1EP_15_1 should be disregarded from further comparisons. A virtually constant moment in this particular specimen is achieved at very small rotations and the strain-hardening effect is nonexistent. This behaviour appears to result from some weld defects that were observed after the test [Girão Coelho et al. 2008].

2. Similarly, test EEP_15_2 is not considered for comparisons in terms of resistance and ductility. The rotational behaviour has a markedly sharp and short plastic plateau (Figure 11a). In this case, the parameter $M_{j,R,exp}$ is not meaningful. In fact, this specimen develop a moment capacity that approaches the code resistance predictions $M_{j,R,EC3}$.
3. In some cases strength predictions are clearly underestimated (ratio $M_{j,R,EC3}/M_{j,R,exp}$ < 0.80). It is likely that this behaviour is related to the experimental computation of the "pseudo-plastic" resistance. Tests FS4a and FS4b produce a ductile moment-rotation behaviour that is characterized by a quite smooth yield plateau, whereas for the remaining tests this plateau shifts up. This may well have an effect on the above definition for $M_{j,R,exp}$.

3.3 Further considerations on the connection ductility

The consistency of the semi-continuous structural modelling of steel frameworks requires the establishment of accurate criteria regarding the rotation capacity and the ductility of the joints. The rotation capacity is the angle through which the joint can rotate for a given resistance level without failing. The ductility properties of a joint reflect the length of the yield plateau of the moment-rotation response. Both criteria should be based on the mechanical and geometrical characteristics of the joint components.

To meet the criterion for rotation capacity, the available connection rotation must be higher than the required joint rotation. For mild steel grades, it is generally accepted that a minimum of 35-40 mrad ensures "sufficient rotation capacity" of a bolted connection in a partial strength scenario. Wilkinson et al. [2006] suggest that a moment connection in steel moment resisting frames in a seismic area must develop a minimum plastic rotation of 30 mrad. The validation of this criterion for high strength steels however requires further investigation. Table 4 computes the experimental values (index "exp") of connection plastic rotation $\phi_{p,u}$, which corresponds to the difference between the ultimate joint rotation ϕ_C and the first yielding rotation ϕ_y [Faella et al. 2000]:

$$\phi_y = \frac{2/3\, M_{j,R}}{S_{j,ini}} \tag{18}$$

Experimental results from tests on end plates made from mild steel S355 (FS1) are also included in this table [Girão Coelho 2004; Girão Coelho et al. 2004, 2006]. Test FS1 uses a similar configuration to test FS4.

Table 3: EN 1993-1-8 predictions of the structural properties of the connections tested and ratio to the experiments

Test ID	**Stiffness** (kNm/mrad)			**Resistance** (kNm)			**Rotation capacity**	
	$S_{j,ini,EC3}$	$S_{j,ini,exp}$	**Ratio**	$M_{j,R,EC3}$	$M_{j,R,exp}$	**Ratio**	$t_{ep,max}$(mm)	**Eq. (12) verifies?**
F1EP_15_1	23.3	18.4	1.27	149	192	0.78	14.78	No. ($t = t_{ep} = 15.30$ mm)
F2EP_15_1	23.9	12.7	1.88	152	128	1.19	14.78	No. ($t = t_{ep} = 15.30$ mm)
EEP_15_1	58.7	30.0	1.96	244	270	0.90	12.05	No. ($t = t_{ep} = 15.25$ mm)
F1EP_15_2	22.6	14.1	1.60	167	175	0.95	11.67	No. ($t = t_{ep} = 14.75$ mm)
F2EP_15_2	21.5	12.3	1.75	164	160	1.03	11.67	No. ($t = t_{ep} = 14.64$ mm)
EEP_15_2	58.0	35.3	1.64	369	245	1.51	11.67	No. ($t = t_{ep} = 14.62$ mm)
F1EP_10_2	12.4	7.8	1.59	104	95	1.09	12.29	Yes. ($t = t_{ep} = 10.15$ mm)
F2EP_10_2	12.4	7.2	1.72	104	89	1.17	12.29	Yes. ($t = t_{ep} = 10.25$ mm)
EEP_10_2a	31.9	17.2	1.85	184	173	1.06	12.29	Yes. ($t = t_{ep} = 10.10$ mm)
EEP_10_2b	34.3	19.9	1.72	184	188	0.98	10.03	No. ($t = t_{ep} = 10.10$ mm)
F1EP_10_3	11.8	9.3	1.27	138	171	0.81	10.53	Yes. ($t = t_{ep} = 10.00$ mm)
F2EP_10_3	12.3	8.0	1.54	140	155	0.90	10.53	Yes. ($t = t_{ep} = 10.00$ mm)
EEP_10_3	31.9	20.7	1.54	247	235	1.05	10.53	Yes. ($t = t_{ep} = 10.00$ mm)
F2EP_10_2(M27)	12.1	7.2	1.68	101	98	1.03	11.71	Yes. ($t = t_{ep} = 10.05$ mm)
EEP_10_2(M27)	32.8	23.2	1.41	184	195	0.94	11.71	Yes. ($t = t_{ep} = 10.10$ mm)
F2EP_10_3(M27)	12.1	10.9	1.11	137	123	1.11	10.03	Yes. ($t = t_{ep} = 10.00$ mm)
EEP_10_3(M27)	32.8	23.0	1.43	247	253	0.98	10.03	Yes. ($t = t_{ep} = 10.03$ mm)
FS4a	*32.8*	*16.2*	*2.02*	*124*	*166*	*0.75*	*8.25*	No. ($t = t_{ep} = 10.06$ mm)
FS4b	*32.8*	*17.1*	*1.92*	*124*	*163*	*0.76*	*8.25*	No. ($t = t_{ep} = 10.06$ mm)

Table 4: Experimental evaluation of the connection ductility indicators and plastic rotation supply

Test ID	$\phi_{y,exp}$ (mrad)	$\phi_{Mj,R,exp}$ (mrad)	$\phi_{Mj,max}$ (mrad)	$\phi_{C,exp}$ (mrad)	$\phi_{p,u,exp}$ (mrad)	R_j	$\vartheta_{j,maxload}$	ϑ_j
F2EP_15_1	7	10	32	40	33	1.34	3.20	4.00
EEP_15_1	6	9	28	28	22	1.21	3.11	3.11
F1EP_15_2	8	12	34	37	29	1.32	2.83	3.08
F2EP_15_2	9	13	33	39	30	1.34	2.54	3.00
F1EP_10_2	8	12	39	46	38	1.49	3.25	3.83
F2EP_10_2	8	12	35	41	33	1.31	2.92	3.42
EEP_10_2a	7	10	36	45	38	1.41	3.60	4.50
EEP_10_2b	6	9	37	46	40	1.34	4.11	5.11
F1EP_10_3	12	*	46	46	34	1.18	—	—
F2EP_10_3	13	*	52	—	—	1.14	—	—
EEP_10_3	8	11	38	38	30	1.39	3.45	3.45
F2EP_10_2(M27)	9	14	38	38	29	1.33	2.71	2.71
EEP_10_2(M27)	6	9	30	52	46	1.36	3.33	5.78
F2EP_10_3(M27)	8	14	42	67	59	1.41	3.00	4.79
EEP_10_3(M27)	7	12	31	44	37	1.24	2.58	3.67
FS1	*5*	*7*	*77*	*111*	*106*	*1.47*	*11.9*	*17.1*
FS4	*7*	*10*	*44*	*64*	*57*	*1.15*	*4.6*	*6.8*

In general, thinner end plates meet the above criterion for the plastic rotation supply. Requirements for ductility ensure that brittle failures are avoided, i.e. the inelastic deformations are sufficiently large. The joint ductility strongly depends on the material performance (for plates and bolts). Nowadays, the quality of high strength steel meets similar standards to mild steel grades. Uniaxial tension tests on high strength steel coupons have shown that these steels can achieve elongations at fracture up to 20%, which is considered excellent [Bjorhovde 2004a; Günther 2005]. However, the assurance of a good material ductility does not necessarily imply that the whole structure will behave ductile. The behaviour of steel is strongly dependent on the load history and the presence of residual strains due to prior occurrence of large deformations.

The ductility can be quantified by means of two performance indicators:

1. resistance index R_j, defined as the maximum joint resistance divided by the pseudo-plastic resistance level:

$$R_j = M_{j,max} / M_{j,R} \tag{19}$$

2. joint ductility index ϑ_j that relates the rotation capacity of the joint ϕ_C to the rotation value corresponding to the joint plastic resistance $\phi_{M_{j,R}}$ [Girão Coelho et al. 2006]:

$$\vartheta_j = \phi_C / \phi_{M_{j,R}} \tag{20}$$

Table 4 evaluates the above indicators for the several specimens. Experimentally, the rotation capacity was defined at the rotation level for which failure of one or more components occurred. Table 4 also includes the rotation values at maximum load and the corresponding ductility levels $\vartheta_{j,max\ load}$:

$$\vartheta_{j,max\ load} = \phi_{M_{j,max}} / \phi_{M_{j,R}} \tag{21}$$

The following conclusions are drawn:

1. Within the same test series, the ductility indicators are similar for both flush end plate configurations; this means that the welding detail did not play an important role in the joint behaviour (Table 4).
2. Bolts 8.8 ensure a more ductile behaviour when compared to bolts 12.9 (see results for specimens EEP_10_2a and EEP_10_2b – the joint ductility index assumes higher values although the resistance indices are similar).
3. The requirement for sufficient joint ductility adopted in EN 1993-1-8, Eq. (12), gives satisfactory results. In fact, the prediction curve adopted in the code agrees well with the experiments (see Figure 12). A trend fit analysis of the experimental data by means of a power function $y = ax^b$, whereby a and b are unknown coefficients, $y = t_{ep}/\phi_b$ and $x = f_{u,b}/f_y$, gives the following trend equation that compares well with Eq. (12). (Figure 12):

$$t_{ep} = 0.358\phi_b \left(f_{u,b}/f_y \right)^{0.5268} \tag{22}$$

4. Experimental observations and statistical data analysis show that the following values for plastic rotation supply and resistance and ductility indicators may be used to lower-bound the requirements for sufficient ductility, according to EN 1993-1-8 (Table 3, column 9):

$$\phi_{p,u,exp} \geq 35 \text{ mrad} \quad \text{and} \quad R_j \geq 1.3 \quad \text{and} \quad \vartheta_j^{\vartheta} \geq 4 \tag{23}$$

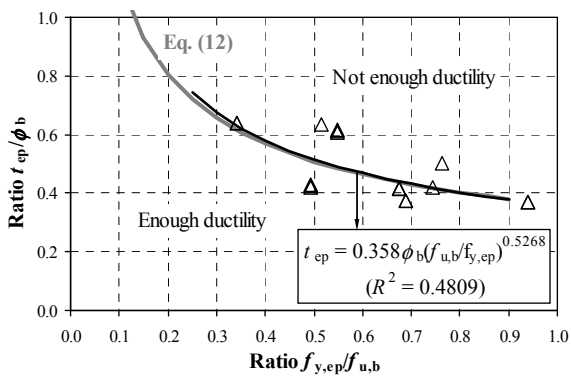

Figure 12: Ductility requirements for specimens employing S690 and S960

4 Behaviour of high strength steel web shear panels

Column web panels are generally classified as "high ductility components" [Girão Coelho 2004; Jaspart 1997]. Failure can develop due to (i) shear yielding and/or (ii) shear buckling of the column web. The first mechanism is intrinsically a stable and ductile failure mode. Web buckling due to shear is essentially a local buckling phenomenon. Typical panels are able to undergo large inelastic distortions before buckling in shear and, consequently, the latter mechanism is usually precluded. Therefore, the panel zones are considered to be a very good source of deformation capacity in steel joints. As a result, EN 1993-1-8 allows inelastic panel zone design procedures. It assumes that the panel behaviour is characterized by an elastic stiffness $K_{wp,el}$, and plastic resistance $V_{wp,Rd}$ that are evaluated as follows:

$$K_{wp,el} = 0.38 A_v E_w \tag{24}$$

whereby A_v is the shear area of the column section and E_w is the Young modulus of the web (web: index "w"; web panel: index "wp"), and:

$$V_{wp,Rd} = \frac{0.9 f_{y,w} A_v}{\sqrt{3}} + \frac{4 M_{pl,f,Rd}}{h_t} \tag{25}$$

where $f_{y,w}$ is the yield stress of the column web, h_t is the height of the panel zone and $M_{pl,f,Rd}$ is the plastic moment resistance of the column flanges. EN 1993-1-8 does not provide an anticipated value of deformation capacity.

The details of an experimental and numerical study for characterization of the force-deformation behaviour of high strength steel web panels carried out at Delft University of Technology can be found in Girão Coelho et al. [2008, 2009]. The following observations were made from this study:

1. The behaviour of nonslender web panels (tests 1 to 7 and 11 to 17) was stable and the decrease in stiffness after yielding was small and gradual (Figure 13). There was a large margin of reserve post-yield strength in the panel zone. The drop in strength was only noticeable at very large inelastic distortions. The behaviour of slender web panels (tests 8 to 9 and 18 to 20) was quite different: the panel can carry additional

load after buckling and have some post-buckling deformation reserve. The drop in strength however occurs at relatively small deformations (Figure 14).

2. Nonslender web panels exhibited a remarkable ductility and underwent very large distortions before failure. It is possible to have deformation capacities above 100 mrad for high strength steel. This characteristic is particularly relevant for the S960 panels. The ductile response results from the progressive shear yielding of the panel.
3. The shear distortion was largest at the centre of the panel and dropped towards the four corners of the panel.
4. The presence of column axial load leads to a drop in strength and ductility of the panels. The tendency of axial load to accelerate the onset of yielding was observed.

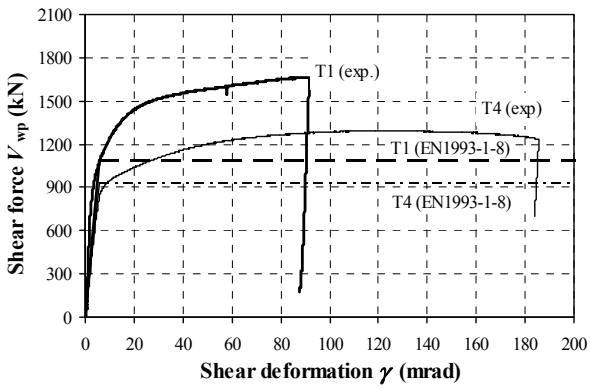

a) Specimens made from S690 (tests 1 to 9)

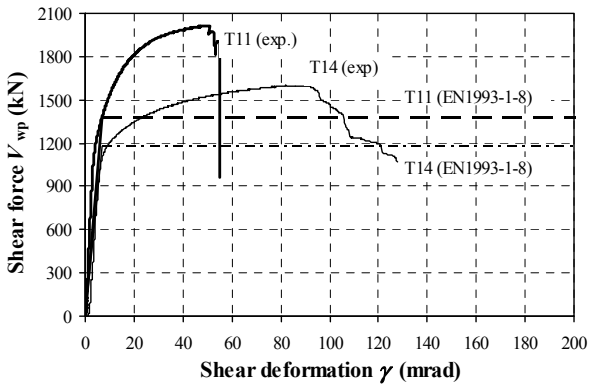

b) Specimens made from S960 (tests 11 to 20)

Figure 13: Shear deformation response of nonslender panels and comparisons with EN 1993-1-8

5. From a design point of view, the bilinear mimicry of the actual response adopted in EN 1993-1-8 provides safe sound results and it is still valid for panels made from steel grades above S460 (Figure 13). EN 1993-1-12 that proposes an elastic design for the web panels can be too conservative.
6. Plastic deformation capacity of the web panel is used as a measure of panel ductility (γ_{pl}) and is evaluated at maximum shear force, max$V$. Nonslender web panels generally achieve plastic rotation supplies above 30 mrad (Table 5). Additionally, two ductility indicators are defined as a means of expressing ductility: (i) the resistance index, $R_{wp} = V_{wp,max}/V_{wp,R}$ and (ii) the ductility index $\mu_{wp} = \gamma_c/\gamma_y$ (section 3.3). Table 5 evaluates these parameters.

5 Discussion and conclusions

This paper presents and discusses the results of an experimental study of end plate bolted connections and web shear panels of beam-to-column joints made from high strength steel. Currently used EN 1993-1-8 and EN 1993-1-12 design criteria for joints are revisited in the light of the available experimental evidence.

The most important conclusions are briefly summarized:

1. Comparison of test results with EN 1993-1-8 procedures for the design of joints within the semi-continuous concept shows that (i) the T-stub idealization of the tension zone of moment connections adopted in EN 1993-1-8 gives accurate results in terms of

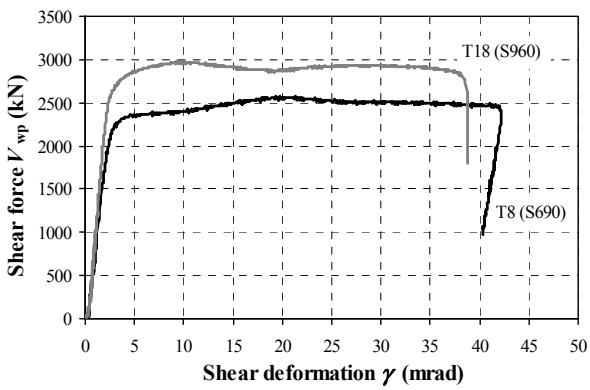

Figure 14: Shear deformation response of slender panels

prediction of the design resistance even when high strength steel grades are employed, (ii) the stiffness properties are overestimated for high strength steel grades and (iii) the guidelines for verification of sufficient rotation capacity are perhaps conservative in some cases but agree well with the experiments.

2. Similar conclusions are drawn for web shear panels [Girão Coelho et al. 2009]. EN 1993-1-8 specifications for the prediction of shear strength and initial stiffness appear to be applicable to panels fabricated from high strength steel.
3. The ductile behaviour of a joint (connections and web shear panel) can be assured by setting requirements to the resistance and ductility indicators defined above, as well as the plastic deformation supply. In addition, the yield stress-to-tensile stress ratio must be limited in order to ensure adequate deformation capacity.

Table 5: Experimental evaluation of the web panel ductility indicators and plastic deformation supply

Test ID *(For Test ID, see [Girão Coelho et al 2008])*	$\gamma_{pl,maxV}$ (mrad)	R_{wp}	$\mu_{wp,maxV}$	μ_{wp}
1	87	1.20	37.5	37.5
2	66	1.09	22.0	29.4
3	32	1.08	18.2	48.7
4	124	1.34	38.1	54.1
5	80	1.13	29.2	55.0
6	111	1.20	35.6	44.1
7	104	1.08	39.7	58.1
8	17	1.11	13.6	30.2
9	16	1.08	14.8	35.3
11	44	1.19	15.5	17.1
12	32	1.07	10.9	14.9
13	22	1.14	10.5	23.0
14	76	1.20	25.0	33.5
15	53	1.05	13.0	20.0
16	74	1.13	16.6	20.4
17	46	1.03	18.3	36.6
18	8	1.08	8.0	30.3
19	15	1.05	11.0	34.4
20	6	1.05	4.8	28.3

The next logical step forward is the numerical analysis of these joint configurations to set up sound design criteria regarding the requirements for deformation capacity and ductility of connections and web panels in order to establish confidence in the inelastic design of high strength steel joints.

Literature

Aggerskov, H. (1977). Analysis of bolted connections subjected to prying. *Journal of the Structural Division ASCE*, 103(ST11): 2145-2163

Beg, D., Zupančič, E., Vayas, I. (2004). On the rotation capacity of moment connections. *Journal of Constructional Steel Research*, 60: 601-620

Bjorhovde, R. (2004a). Development and use of high performance steel. *Journal of Constructional Steel Research*, 60: 393-400

Bjorhovde, R. (2004b). Deformation considerations for connection performance and design. *Proceedings of the Fifth International ECCS/AISC Workshop on Connections in Steel Structures: Innovative Steel Connections* (Eds.: F.S.K. Bijlaard, A.M. Gresnigt and G.J. van der Vegte), Amsterdam, 11-20

European Committee for Standardization (CEN). (2005a). EN 1993-1-1 – Eurocode 3: *Design of Steel Structures* – Part 1-1: *General Rules and Rules for Buildings*

European Committee for Standardization (CEN). (2005b). EN 1993-1-8 – Eurocode 3: *Design of steel structures* – Part 1-8: *Design of joints*

European Committee for Standardization (CEN). (2005c). EN 1993-1-12 – Eurocode 3: *Design of steel structures* – Part 1-12: *Additional rules for the extension of EN 1993 up to steel grades S700*

Faella, C., Piluso, V., Rizzano, G. (2000). *Structural semi-rigid connections – theory, design and software*, CRC Press

Gioncu, V., Mateescu, G., Petcu, D., Anastasiadis, A. (2000). Prediction of available ductility by means of local plastic mechanism method: DUCTROT computer program. Chapter 2.1 in *Moment Resistant Connections of Steel Frames in Seismic Areas* (Ed.: F Mazzolani), E&FN Spon, 95-146

Girão Coelho, A.M. (2004). *Characterization of the ductility of bolted end plate beam-to-column steel connections*. PhD Thesis, University of Coimbra. Free download at: http://www.cmm.pt/gcom/publicacoes/teses/phd_thesis_ana_girao.pdf

Girão Coelho, A.M., Bijlaard, F.S.K. (2006). *Experimental behaviour of high performance steel moment connections*. Report 6-06-5, Faculty of Civil Engineering, Stevin Laboratory – Steel Structures, Delft University of Technology

Girão Coelho, A.M., Bijlaard, F.S.K. (2007). Experimental behaviour of high strength steel end plate connections. *Journal of Constructional Steel Research*, 63: 1228-1240

Girão Coelho, A.M., Bijlaard, F.S.K., Simões da Silva, L. (2004). Experimental assessment of the ductility of extended end plate connections. *Engineering Structures*, 26: 1185-1206

Girão Coelho, A.M., Simões da Silva, L., Bijlaard, F.S.K. (2006). Ductility analysis of bolted extended end plate beam-to-column connections in the framework of the component method. *Steel and Composite Structures*, 6(1): 33-53

Girão Coelho, A.M., Bijlaard, F.S.K., Kolstein, H. (2008). *Behaviour of high strength steel web shear panels*. Report 6-07-2, Faculty of Civil Engineering, Stevin Laboratory – Steel Structures, Delft University of Technology

Girão Coelho, A.M., Bijlaard, F.S.K., Kolstein, H. (2009). Experimental behaviour of high-strength steel web shear panels. *Engineering Structures*, (in press, doi:10.1016/j.engstruct.2009.02.023

Günther, H-P. (Ed.) (2005). *Use and application of high-performance steels for steel structures*. International Association for Bridge and Structural Engineering (IABSE), Structural Engineering Documents, Vol. 8

Huber, G., Tschemmernegg, F. (1998). Modelling of beam-to-column joints. *Journal of Constructional Steel Research*, 45: 199-216

Jaspart, J.P. (1991). *Étude de la semi-rigidité des noeuds pouter-colonne et son influence sur la resistance et la stabilité des ossatures en acier*. PhD thesis (in French), University of Liège

Jaspart, J.P. (1997). *Contributions to recent advances in the field of steel joints – column bases and further configurations for beam-to-column joints and beam splices*. Professorship Thesis, University of Liège

Packer, J.A., Morris, L.J. (1977). A limit state design method for the tension region of bolted beam-to-column connections. *The Structural Engineer*, 55(10): 446-458

Weynand, K., Jaspart, J.P., Steenhuis, M. (1995). The stiffness model of revised Annex J of Eurocode 3. In: *Proceedings of the Third International Workshop on Connections in Steel Structures III, Behaviour, Strength and Design* (Eds.: R Bjorhovde, A Colson and R Zandonini), Trento, 441-452

Wilkinson, S., Hurdman, G., Crowther, A. (2006). A moment resisting connection for earthquake resistant structures. *Journal of Constructional Steel Research*, 62: 295-302

Yee Y.L., Melchers, R.E. (1986). Moment-rotation curves for bolted connections. *Journal of Structural Engineering ASCE*, 112(3): 615-635

Zoetemeijer, P. (1974). A design method for the tension side of statically loaded, bolted beam-to-column connections. *Heron*, 20(1): 1-59

Zoetemeijer, P. (1990). *Summary of the research on bolted beam-to-column connections*. Report 25-6-90-2, Faculty of Civil Engineering, Stevin Laboratory – Steel Structures, Delft University of Technology